



Published in final edited form as:

*Circ Res.* 2014 January 17; 114(2): 295–306. doi:10.1161/CIRCRESAHA.114.302857.

## Cardiac Myocyte Z-line Calmodulin is Mainly RyR2-Bound and Reduction is Arrhythmogenic and Occurs in Heart Failure

Yi Yang<sup>1</sup>, Tao Guo<sup>1</sup>, Tetsuro Oda<sup>1</sup>, Asima Chakraborty<sup>2</sup>, Le Chen<sup>3</sup>, Hitoshi Uchinoumi<sup>1</sup>, Anne A. Knowlton<sup>1,3</sup>, Bradley R. Fruen<sup>4</sup>, Razvan L. Cornea<sup>4</sup>, Gerhard Meissner<sup>2</sup>, and Donald M. Bers<sup>1</sup>

<sup>1</sup>Department of Pharmacology, University of California, Davis, CA

<sup>2</sup>Department of Biochemistry and Biophysics, University of North Carolina, Chapel Hill, NC

<sup>3</sup>Molecular and Cellular Cardiology Division, Department of Medicine, University of California, Davis, CA

<sup>4</sup>Department of Biochemistry, Molecular Biology and Biophysics, University of Minnesota, Minneapolis, MN.

### Abstract

**Rationale**—Calmodulin (CaM) associates with cardiac ryanodine receptors (RyR2) as an important regulator. Defective CaM-RyR2 interaction may occur in heart failure (HF), cardiac hypertrophy, and catecholaminergic polymorphic ventricular tachycardia (CPVT). However, the in situ binding properties for CaM-RyR2 are unknown.

**Objective**—We sought to measure the in situ binding affinity and kinetics for CaM-RyR2 in normal and HF ventricular myocytes, estimate the percentage of Z-line localized CaM that is RyR2-bound and test cellular function of defective CaM-RyR2 interaction.

**Methods & Results**—Using FRET (fluorescence resonance energy transfer) in permeabilized myocytes, we specifically resolved RyR2-bound CaM from other potential binding targets, and measured CaMRyR2 binding affinity in situ ( $K_d = 10\text{--}20$  nM). Using RyR2<sup>ADA/+</sup> knock-in (KI) mice, in which half of the CaM-RyR2 binding is suppressed, we estimated that >90% of Z-line CaM is RyR2-bound. Functional tests indicated a higher propensity for Ca<sup>2+</sup> waves production and stress induced ventricular arrhythmia in RyR2<sup>ADA/+</sup> mice. In a post myocardial infarction (MI) rat HF model, we detected a decrease in the CaMRyR2 binding affinity ( $K_d \approx 51$  nM, ~3 fold increase) and unaltered FKBP12.6-RyR2 binding affinity ( $K_d \approx 0.8$  nM).

**Conclusions**—CaM binds to RyR2 with high affinity in cardiac myocytes. Physiologically, CaM is bound to >70% of RyR2 monomers and inhibits SR Ca<sup>2+</sup> release. RyR2 is the major binding site for CaM along the Z-line in cardiomyocytes and dissociating CaM from RyR2 can cause severe ventricular arrhythmia. In HF, RyR2 shows decreased CaM affinity, but unaltered FKBP12.6 affinity.

**Address correspondence to:** Dr. Donald M. Bers Department of Pharmacology University of California, Davis Davis, CA 95616 Tel: (530) 752-3200 Fax: (530) 752-7710 dmbers@ucdavis.edu.

DISCLOSURES

None.

## Keywords

CaM; FKBP12.6; FRET; binding properties; RyR2; CPVT; heart failure; fluorescent imaging; ryanodine receptor; arrhythmia

---

## INTRODUCTION

Approximately 50% of heart failure (HF) patients die of ventricular arrhythmia and sudden cardiac death<sup>1</sup>. It is known that ryanodine receptor type 2 (RyR2) mediated Ca<sup>2+</sup> leak from the sarcoplasmic reticulum (SR) during diastole can activate inward current via Na/Ca exchange (NCX)<sup>2</sup> and evoke delayed afterdepolarizations (DADs). In HF, there is enhanced diastolic SR Ca<sup>2+</sup> leak via RyR2 and other electrophysiological changes that greatly enhance the propensity for DADs and triggered cardiac arrhythmias, a leading cause of ventricular tachyarrhythmia and sudden cardiac death.<sup>3-6</sup> Thus, RyR2 has emerged as a potential therapeutic target for treating HF and arrhythmia. Stabilizing RyR2 and preventing abnormal Ca<sup>2+</sup> leak (without affecting normal excitation-contraction coupling) may be a valid therapeutic approach.

Calmodulin (CaM) is an important RyR2 regulator, but has multiple cellular targets. CaM has two pairs of globular Ca<sup>2+</sup> binding E-F hand domains connected by a flexible linker.<sup>7</sup> At high [Ca<sup>2+</sup>], Ca<sup>2+</sup> binds cooperatively to CaM inducing a conformational change that translates intracellular [Ca<sup>2+</sup>] signals to diverse processes via many targets, including: myosin light chain kinase, calcineurin, nitric-oxide synthase, phosphodiesterase, adenylyl cyclase, Ca<sup>2+</sup>/CaM-dependent kinase (CaMK), Ca<sup>2+</sup>-activated potassium channels, L-type Ca<sup>2+</sup> channels (LTCCs), and RyRs.<sup>8-11</sup>

CaM binds to RyR2 stoichiometrically (four CaMs per tetrameric RyR2) and amino acids 3583-3603 on RyR2 are essential for this interaction.<sup>12-14</sup> CaM inhibits RyR2 opening at all [Ca<sup>2+</sup>] and as such may be a critical regulator of SR Ca<sup>2+</sup> release.<sup>13,14</sup> Cryo-EM based three-dimensional reconstruction studies showed that Ca<sup>2+</sup>-free CaM (apoCaM) binds in the RyR cytosolic domain 3, within 60-70Å from FKBP12.6 bound on the same RyR face,<sup>15,16</sup> and we have demonstrated that fluorescence resonance energy transfer (FRET) can be measured between these partners bound to either RyR1 or RyR2.<sup>17,18</sup> FKBP12.6 was reported to bind RyR2 tightly as an important regulator in RyR2 gating but aspects of the FKBP12.6-RyR2 interaction and function remain controversial.<sup>19-22</sup> It was also reported that CaM could stabilize the RyR2 in the closed state during diastole and facilitate the termination of Ca<sup>2+</sup> release by decreasing the probability of channel reopening and prolonging the closed time.<sup>23</sup> Defective CaM-RyR2 interaction has potentially broad implication in cardiac pathology. Mutations of critical residues in the highly conserved CaM binding region can severely decrease, or abolish CaM binding to RyR2 and cause severe hypertrophic cardiomyopathy and early death in animals.<sup>13,24</sup> In non-ischemic HF animal models, CaM binding to RyR2 was decreased.<sup>25,26</sup> A recent study indicates that defective CaM binding to RyR2 is also involved in catecholaminergic polymorphic ventricular tachycardia (CPVT)-associated RyR2 dysfunction.<sup>27</sup> So, the CaM-RyR2 interaction may be critical for arrhythmias and HF pathogenesis.

Here, we used FRET to resolve RyR-bound CaM from other CaM targets, and in the native myocyte environment, to characterize CaM-RyR2 interaction properties for normal and HF cardiomyocytes. Knock-in (KI) heterozygous mice (RyR2<sup>ADA/+</sup>),<sup>13</sup> with genetically disrupted CaM-RyR2 association (W3587A/L3591D/F3603A) were used to estimate what percentage of Z-line bound CaM is RyR2-bound, and test for increased arrhythmia susceptibility in both myocytes and intact animals under acute stress. This would be analogous to what is seen in CPVT, which is linked to RyR2 mutations.<sup>28,29</sup> This ADA mutant RyR2 is not expected to change CaM effects at other CaM targets. Human mutations in CaM have recently also been associated with CPVT, which may be partially recapitulated by these RyR2<sup>ADA/+</sup> mice.<sup>30</sup>

## METHODS

Ventricular myocytes were isolated as previous described,<sup>22</sup> from hearts of WT or RyR2<sup>ADA/+</sup> KI mice and Sprague-Dawley rats (control and 12 weeks after HF induced by coronary ligation<sup>31,32</sup>). FKBP12.6 and CaM were labeled with Alexa Fluor 488 and 568 (AF488 and AF568) as described, which bind to and regulate RyRs in SR like wild type proteins.<sup>17,18</sup> Some myocytes were saponin-permeabilized and bathed in physiological internal solutions. Fluorescent FKBP12.6 and CaM (F-FKBP and F-CaM) and 25  $\mu$ M Fluo-4 (to measure [Ca]<sub>i</sub>) were used with confocal imaging.<sup>22,33</sup> ECGs were recorded in RyR2<sup>ADA/+</sup> and WT mice during isoproterenol (ISO, 2mg/kg) and caffeine (120mg/kg) challenges. Further details are in the Online Methods.

## RESULTS

### Steady-state binding of CaM to RyR2

**Pre-depletion of endogenous CaM by suramin**—RyR2s are concentrated at Z-lines, which is also true for CaM,<sup>34</sup> and ~90% of apoCaM binding sites are occupied by endogenous CaM.<sup>34</sup> Online Fig. IAi shows the F-CaM Z-line striation pattern after 60 nM F-CaM was washed in. Suramin (5  $\mu$ M) wash-in abolished striations within 60 s (Online Fig. IAii), indicating F-CaM dissociation from Z-line sites. After suramin-dependent stripping and subsequent wash-out (20 min), F-CaM rebound at Z-lines, restoring striations (Online Fig. IAiii). Before suramin treatment, F-CaM binding kinetics were slow, time constant  $\tau$  = 11.5 min (Online Fig. IB) which represents F-CaM replacing endogenous RyR-bound CaM.<sup>34</sup> After depleting endogenous RyR-bound CaM with suramin, F-CaM binding was much faster ( $\tau$  = 2 min; Online Fig. IC), reflecting F-CaM binding to unoccupied binding sites.  $B_{\max}$  was not significantly altered by suramin pretreatment, indicating that suramin completely depleted endogenous Z-line bound CaM, and that CaM and suramin binding are completely reversible.

**Steady-state CaM-RyR2 binding affinity**—Strong FRET between F-FKBP and F-CaM is effective in distinguishing CaM bound to RyR2 vs. other CaM targets.<sup>18</sup> After suramin pretreatment, 100 nM F-FKBP (donor) was washed-in to saturate FKBP binding sites on RyR2.<sup>18,22</sup> Then different F-CaM (acceptor) concentrations were washed-in and allowed to reach steady state (20-120 min). RyR2-bound CaM is detected through FRET by sensitized emission (SE). Fig. 1A shows fluorescent striations with F-FKBP excitation at 488 nm and

two different [F-CaM] in both donor (green) and acceptor (red) channels. In FRET-based  $K_d$  measurements, as [F-CaM] increases, donor fluorescence decreases (donor quench), while acceptor fluorescence increases (enhanced acceptor fluorescence, EAF). The fluorescence intensity in the acceptor channel (difference between Z- and M-line fluorescence) is due to EAF (FRET) and reflects the amount of CaM specifically bound to RyR2. The binding isotherm in Fig. 1B, is well described by a specific binding curve with a single binding site ( $K_d = 18 \pm 2$  nM). We also calculated  $K_d$  from donor quenching ( $21 \pm 3$  nM; Online Fig. II) in agreement with that.

To test whether FRET occurs between one donor and one acceptor, in Fig. 1C we plotted donor signal (y-axis) vs. acceptor signal (x-axis) for the same [F-CaM], from experiments shown in Fig 1B. The dependence of donor fluorescence (F-FKBP; decreasing due to FRET) on the acceptor fluorescence (FCaM; increasing FRET) is linear, consistent with bimolecular FRET.<sup>35</sup> This suggests that FRET is exclusively between FKBP12.6 and CaM bound to the same face of the RyR2 (not to another nearby site).<sup>18</sup>

**Total CaM at Z-line**—Using direct F-CaM excitation (543 nm) rather than FRET, we also measured the apparent  $K_d$  for total CaM bound at the Z-line (i.e., CaM bound to RyR2 plus other sites along the Z-line). Fig. 1D shows the Z-line striations at two different [F-CaM]. The plot of peak height reveals a single saturable binding component for F-CaM at the Z-line with  $K_d = 17 \pm 2$  nM (Fig. 1E).  $K_d$  values for RyR2-bound CaM (Fig. 1B) and for total CaM bound at the Z-line (Fig. 1E) are very similar. One possible explanation is that RyR2 is the quantitatively dominant CaM binding site in the Z-line. The other is that several CaM binding sites have similar affinities. Through linear bath [F-CaM] calibration (Fig. 1F), we can infer the concentration of Z-line bound F-CaM in permeabilized myocytes. The maximum bound CaM at the Z-lines ( $B_{max}$ , Fig. 1E) is  $1.2 \mu\text{M}$ , similar to our prior work,<sup>36</sup> and consistent with the  $B_{max}$  for FKBP12.6 in rat myocytes.<sup>22</sup>

## Kinetics of CaM binding to RyR2

### FRET-based measurement of $k_{on}$ and $k_{off}$ during wash-in/out in myocytes—

After CaM depletion, permeabilized myocytes were saturated with F-FKBP (100 nM). Using FRET, we characterized CaM-RyR2 association ( $k_{on}$ ) and dissociation ( $k_{off}$ ) rate constants in F-CaM wash-in/out experiments (Fig. 2A). During wash-out, fluorescent striations gradually dissipated along a single-exponential decay ( $\tau = 4.5$  min), which corresponds to  $k_{off} = 0.22 \pm 0.01 \text{ min}^{-1}$  ( $n=5$ ). For wash-in, CaM-RyR2 association rate is a function of  $k_{on}$ ,  $k_{off}$  and [F-CaM] ( $k_{wash-in} = k_{on} [\text{CaM}] + k_{off}$ ). Using the  $k_{off}$  above and the wash-in data, we calculated  $k_{on} = 18.9 \pm 1.6 \times 10^6 \text{ min}^{-1}\text{M}^{-1}$  ( $n=5$ ). These  $k_{on}$  and  $k_{off}$  values correspond to  $K_d = 12 \pm 1$  nM ( $k_{off}/k_{on}$ ), which agrees with the steady-state binding results above.

**FRAP-based measurement of  $k_{on}$  and  $k_{off}$  in myocytes**—Permeabilized myocytes were first equilibrated with saturating F-FKBP (100nM) and with [FCaM] in the  $K_d$  range. After photobleaching the acceptor by 543 nm excitation in the central region of the cell (Fig. 2B), we monitored striation recovery (FRAP). FRAP reflects recovery of CaM-RyR2 binding, in which the photobleached RyR-bound F-CaM dissociates and is replaced by fresh

F-CaM from the bath. In Fig. 2C,  $k_{\text{FRAP}}$  was fit to a single-exponential function for two different bath [F-CaM], upon which FRAP is dependent ( $k_{\text{FRAP}} = k_{\text{on}}[\text{F-CaM}] + k_{\text{off}}$ ). The values of  $k_{\text{on}}$  and  $k_{\text{off}}$  are obtained from linear regressions (Fig. 2D). Both  $k_{\text{on}} = 14.5 \pm 2.5 \times 10^6 \text{ min}^{-1} \text{ M}^{-1}$  and  $k_{\text{off}} = 0.144 \pm 0.05 \text{ min}^{-1}$  agree well with the wash-in/out experiments (Fig. 2A), and give a similar  $K_d$  ( $10 \pm 2 \text{ nM}$ ).

**Percentage of total Z-line CaM that is RyR2-bound**—KI mice with genetically disrupted CaM-RyR2 interaction are used here (along with WT mice) to estimate the percentage of total Z-line-bound CaM that is RyR2-bound. These KI mice express RyR2 with a triple-mutation (RyR2-W3587A/L3591D/F3603A, RyR2<sup>ADA/+</sup>) that prevents high-affinity binding of CaM.<sup>13</sup> Homozygous (RyR2<sup>ADA/ADA</sup>) mice all die within 16 days of birth with a severe HF phenotype, loss of T-tubule/junctional couplings and ~70% decrease in RyR2 expression, making them unsuitable here.<sup>13,24</sup> However, the heterozygous mice (RyR2<sup>ADA/+</sup>) have no evidence of HF or structural defects, and exhibit normal life-span and RyR2 expression levels.<sup>13</sup> We find that RyR2<sup>ADA/+</sup> myocytes exhibit reduced F-CaM binding both to the RyR2 (by FRET), and at the Z-line (by direct F-CaM excitation; Fig. 3A,B). For RyR2<sup>ADA/+</sup>, there is a  $50\% \pm 2\%$  reduction in FRET at saturating [F-CaM] ( $\text{FRET}_{\text{max}}$ ), with no significant change in  $K_d$  (Fig. 3C). That fits the expectation that in RyR2<sup>ADA/+</sup> mice ~50% of the RyR2 monomers have the triple-mutation and defective CaM binding. There is also a  $46\% \pm 2\%$  reduction of total CaM at the Z-line (Fig. 3D), which is therefore primarily due to the 50% decrease in CaM binding to RyR2. This suggests that ~92% of Z-line localized CaM is bound to RyR2. We also measured RyR2 monomer expression as total binding ( $B_{\text{max}}$ ) of FKBP12.6 (Online Fig. III).<sup>22</sup> FKBP12.6 binding was identical in RyR2<sup>ADA/+</sup> vs. WT myocytes, confirming an unaltered total number of RyR2 monomers, in line with unaltered  $B_{\text{max}}$  of [<sup>3</sup>H]-ryanodine binding in these mice.<sup>13</sup>

**Ca<sup>2+</sup> sparks in permeabilized RyR2<sup>ADA/+</sup> KI mouse myocytes**—Saponin-permeabilized myocytes are powerful tools for the evaluation of diastolic SR Ca<sup>2+</sup> leak. The free [Ca]<sub>i</sub> can be tightly controlled and it avoids complications due to LTCCs, which can trigger RyR2-mediated Ca<sup>2+</sup> release. However, a potential disadvantage of this method is that some cellular contents (like endogenous proteins) can be lost due to wash-off. Since the endogenous CaM associated with RyR2 may be washed off within 10 min (Fig 2A), we modified the permeabilization protocol, for Ca<sup>2+</sup> spark measurements, to limit this disadvantage. For Ca<sup>2+</sup> spark measurements, myocytes were exposed to saponin (50 μg/ml) for only 20-30 s instead of the 3 min used above for CaM wash-in. Online Fig. IV shows that after 20-30 s permeabilization, Ca<sup>2+</sup> sparks were readily detected in myocytes after 20 min exposure to F-FKBP, F-CaM and fluo-4. However, there was no visible striated pattern observable for F-FKBP, F-CaM, or FRET. This indicates that fluo-4 can enter the cell with this gentler permeabilization, but proteins (e.g. CaM and FKBP12.6) cannot. With the 3 min permeabilization protocol, both FRET striation pattern and Ca<sup>2+</sup> sparks were detected, indicating that all 3 probes entered the cell. This shows that 20-30 s permeabilization can also effectively limit FKBP12.6 and CaM wash-out during the time of Ca<sup>2+</sup> spark measurement. Thus, we can make the Ca<sup>2+</sup> spark measurement in the relatively native cellular environment with respect to CaM and FKBP12.6 concentrations.

Using this approach, we measured diastolic SR  $\text{Ca}^{2+}$  leak as  $\text{Ca}^{2+}$  sparks within 15-20 min of permeabilization. Fig. 4A, B shows that, at 50 nM  $[\text{Ca}^{2+}]_i$ , spark frequency was significantly higher in  $\text{RyR2}^{\text{ADA}/+}$  versus WT mice ( $8.9 \pm 0.3$  vs.  $6.4 \pm 0.5$   $\text{s}^{-1}$  per 100  $\mu\text{m}$ ), which tended to lower SR  $\text{Ca}^{2+}$  content in  $\text{RyR2}^{\text{ADA}/+}$  versus WT (albeit insignificantly; Fig. 4B).  $\text{Ca}^{2+}$  spark frequency depends steeply on SR  $\text{Ca}^{2+}$  content,<sup>37</sup> such that the new steady state spark frequency underestimates the magnitude of the primary effect. The increased  $\text{Ca}^{2+}$  spark frequency could not be prevented by the specific CaMKII inhibitor AIP (Fig. 4B), ruling out a contribution of CaMKII. These results are consistent with half of the RyR2 monomers lacking CaM, allowing higher RyR2 activity.

In a second series of spark experiments we compared the effect of endogenous CaM (as above) with CaM washout and re-admission in WT and  $\text{RyR2}^{\text{ADA}/+}$  mice (Online Fig. V). For WT CaM, wash-off increased  $\text{Ca}^{2+}$  spark frequency,  $\text{Ca}^{2+}$  spark full duration at half-maximum (FDHM), and full width at half-maximum (FDHM). These effects were reversed with CaM re-addition. However, in  $\text{RyR2}^{\text{ADA}/+}$  myocytes the baseline  $\text{Ca}^{2+}$  spark frequency, FDHM and FWHM were already high (comparable to that in CaM-free WT myocytes), and were not influenced by CaM washout or re-admission. Thus, even 500 nM CaM cannot reverse the high  $\text{Ca}^{2+}$  spark frequency caused by defective CaM-RyR2 interaction (Online Fig. V).

We also increased intracellular  $[\text{Ca}^{2+}]_i$  to 100 nM, close to the threshold for  $\text{Ca}^{2+}$  waves in WT mouse myocytes, to further test the propensity for DADs or arrhythmogenesis. The increased  $[\text{Ca}^{2+}]_i$  mimics a  $\text{Ca}^{2+}$  loading stress in permeabilized cells, since both cytosolic and SR  $\text{Ca}^{2+}$  load are increased. In  $\text{RyR2}^{\text{ADA}/+}$  mice ~90% of myocytes produced  $\text{Ca}^{2+}$  waves vs. only ~10% of myocytes for WT mice (Fig. 4C-D), again without a significant difference in  $\text{Ca}^{2+}$  SR load (Fig. 4D). The caffeine-induced  $\text{Ca}^{2+}$  transients were induced during sweeps where no waves occurred, to limit underestimation of SR  $\text{Ca}^{2+}$  content that would occur in the wake of a wave. All these data indicate that the ADA CaM-binding mutation in RyR2, increases diastolic SR  $\text{Ca}^{2+}$  leak under resting conditions, and increases propensity for arrhythmogenic  $\text{Ca}^{2+}$  wave production under moderate  $\text{Ca}^{2+}$  loading conditions.

**$\text{Ca}^{2+}$  transients in  $\text{RyR2}^{\text{ADA}/+}$  KI mouse in intact myocytes**—We also measured  $\text{Ca}^{2+}$  transients in intact ventricular myocytes (Fig. 5A) with or without isoproterenol (ISO, 50 nM) present, and SR  $\text{Ca}^{2+}$  content was evaluated through rapid caffeine application. In 1 Hz field stimulation at baseline,  $\text{RyR2}^{\text{ADA}/+}$  myocytes behave similar to WT in  $\text{Ca}^{2+}$  transient amplitude, time constant of  $\text{Ca}^{2+}$  transient decline, SR  $\text{Ca}^{2+}$  content, and fractional SR  $\text{Ca}^{2+}$  release (Fig. 5B-E). While exposure to ISO (50 nM) had similar effects on  $\text{Ca}^{2+}$  transient amplitude in both WT and  $\text{RyR2}^{\text{ADA}/+}$ , the time constant of  $[\text{Ca}^{2+}]_i$  decline was longer, SR  $\text{Ca}^{2+}$  content was lower and fractional SR  $\text{Ca}^{2+}$  release was increased in  $\text{RyR2}^{\text{ADA}/+}$  vs. WT (Fig 5C-E). The more sensitive  $\text{RyR2}^{\text{ADA}/+}$  and higher  $\text{Ca}^{2+}$  loading in 50 nM ISO may cause the prolonged twitch  $[\text{Ca}^{2+}]_i$  decline (delayed shut-off of release, as demonstrated under analogous conditions in CaMKII $\delta_C$  overexpressing mice that lack phospholamban<sup>38</sup>). The exacerbated leak in  $\text{RyR2}^{\text{ADA}/+}$  mice may also limit the rise in SR  $\text{Ca}^{2+}$  content induced by ISO, like the reduced maximal achievable SR  $\text{Ca}^{2+}$  content in HF or ISO treated myocytes.<sup>24,39</sup> Figure 6 also shows that in  $\text{RyR2}^{\text{ADA}/+}$  myocytes, ISO

increased the propensity for  $\text{Ca}^{2+}$  waves that trigger action potentials. That is, the transition from  $\text{Ca}^{2+}$  wave to spatially synchronized global  $\text{Ca}^{2+}$  release was necessarily synchronized by a triggered action potential. These triggered events could reflect increased arrhythmogenic risk in  $\text{RyR2}^{\text{ADA}/+}$  mice, analogous to CPVT.

**Ventricular arrhythmia in  $\text{RyR2}^{\text{ADA}/+}$  KI mouse**—To test whether the  $\text{RyR2}^{\text{ADA}/+}$  KI mice are more susceptible to CPVT-like arrhythmias, we measured ECGs in intact mice during injection of ISO plus caffeine as has been done in CPVT mouse models.<sup>40</sup> Figure 7A shows that  $\text{RyR2}^{\text{ADA}/+}$  KI mice developed severe stress inducible ventricular arrhythmia. All  $\text{RyR2}^{\text{ADA}/+}$  mice exhibited sustained bigeminy (>20min), a precursor for ventricular tachycardia (VT, Fig 7B). In 60% of  $\text{RyR2}^{\text{ADA}/+}$  mice, bidirectional VT was induced (Fig 7B), and episodes of VT were frequent (4.5/mouse) in  $\text{RyR2}^{\text{ADA}/+}$  mice. In contrast, none of the WT mice exhibited inducible arrhythmia in this protocol.

**Binding affinity of CaM/FKBP12.6 to RyR2 in HF myocytes**—We measured CaM-RyR2 affinity in a rat HF model induced by coronary ligation. Twelve weeks post-infarct these rats exhibit increased heart/body weight ratio, increased LV diastolic dimensions (LVDD) and decreased fractional shortening.<sup>31,32</sup> Other HF molecular markers (ANP, BNP, TNF- $\alpha$ ) are also increased in this model.<sup>32</sup> The HF rats used here had reduced fractional shortening (<20% vs. normal: 46%) and elevated LVDD (see Online Fig. VI). We used FRET to measure the CaM-RyR2 affinity. In HF vs. normal myocytes, the CaM-RyR2 affinity was ~3-fold lower ( $K_d=51\pm 4$  nM; Fig. 8A). We also performed paired experiments with sham rats, with [F-CaM] near the  $K_d$  and saturating ( $\text{FRET}_{\text{max}}$ ) (Fig 8B). At [F-CaM] near WT  $K_d$ , changes in affinity are readily detected, and binding was significantly lower in HF.  $\text{FRET}_{\text{max}}$  was unaltered.

FKBP12.6 was suggested to also be a critical RyR2 stabilizer, with decreased affinity in HF (although this is controversial).<sup>41</sup> Using methods previously described,<sup>22</sup> we measured, for the first time within HF myocytes, the FKBP12.6-RyR2 affinity ( $K_d = 0.8 \pm 0.1$  nM; Fig. 8C). This is almost identical to the  $K_d$  we previously measured in normal rat myocytes under the same conditions ( $0.7 \pm 0.1$  nM).<sup>21</sup> We also performed paired experiments (as for CaM). We found no significant changes in FKBP12.6-RyR2 binding either at subsaturating or saturating [F-FKBP] in sham vs. HF rat myocytes (Fig. 8D).

## DISCUSSION

Here we resolved CaM binding to RyR2 vs. other Z-line binding partners, and characterized CaM-RyR2 binding properties ( $K_d$  and on/off rates) in permeabilized ventricular myocytes by 3 independent methods (Online table I).  $\text{RyR2}^{\text{ADA}/+}$  KI mice with disrupted CaM-RyR2 binding, were used to determine that >90% of Z-line CaM is bound to RyR2. Functional consequences of reduced CaM binding to RyR2 were detected using  $\text{Ca}^{2+}$  measurements in WT vs.  $\text{RyR2}^{\text{ADA}/+}$  KI myocytes, with CaM wash-out from WT myocytes, and arrhythmogenesis tests in mice. We also found CaM-RyR binding affinity to be reduced in HF myocytes. These results provide important new insights into understanding CaM-RyR2 interactions in normal and HF myocytes.

## CaM-RyR2 binding properties in myocytes

CaM, as a key regulator of RyR2 function, may be important in myocyte  $\text{Ca}^{2+}$  homeostasis in HF, cardiac hypertrophy, and CPVT. But in situ CaM-RyR2 binding properties were previously unknown. Using three independent methods, we demonstrated that CaM binds to RyR2 with high affinity ( $K_d=10\text{-}20\text{ nM}$ ) in myocytes at  $50\text{ nM } [\text{Ca}^{2+}]_i$ . Considering the measured free [CaM] in myocytes ( $50\text{-}75\text{ nM}$ ),<sup>34</sup> the majority of RyR2 monomers ( $\sim 70\text{-}90\%$ ) have CaM bound, such that CaM can influence local  $[\text{Ca}^{2+}]_i$  by inhibiting RyR2 opening at physiological  $[\text{Ca}^{2+}]_i$ .<sup>12-14,23,26,42</sup> The CaM-RyR2 binding affinity we measured in myocytes is higher than in cell lysates and SR vesicles.<sup>17,27</sup> This could be due to differences in experimental conditions or subcellular fractionation effects. In SR vesicles, essential partners from the cellular environment may be lost, or post-translational modifications of RyR2 might occur (e.g., phosphorylation or oxidation), which can alter CaM-RyR2 affinity.<sup>23,43</sup> Using three methods, we measured very similar CaM-RyR2 affinities that are consistent with CaM's physiological function.<sup>13,23</sup> This supports that our  $K_d$  measurements ( $10\text{-}20\text{ nM}$ ) are valid for the CaM-RyR2 binding affinity in the native cardiac myocyte environment.

According to our data, CaM-RyR2 has a relatively slow  $k_{\text{off}}$  ( $\sim 0.2\text{ min}^{-1}$ ), meaning that the average dwell-time for CaM on RyR2 is  $\sim 5\text{ min}$ , under resting conditions. In addition, high  $[\text{Ca}^{2+}]_i$  ( $500\text{ nM}$ ) strengthens CaM binding to RyR/Z-lines and greatly slows CaM dissociation.<sup>18,34</sup> Hence, increased CaM-RyR2 affinity during the  $\text{Ca}^{2+}$  transient ( $<1\text{ s}$ ) would further enhance CaM saturation at all RyR2 monomers in the physiological beat-to-beat situation. Furthermore, it was proposed that CaM can switch between two binding sites separated by  $\sim 33\text{ \AA}$  on RyR1 during each cardiac cycle.<sup>44,45</sup> The two-site switch involves two sets of association and dissociation process, which seems unlikely to occur within the very short systolic time, according to our measured kinetics. Taken together, these suggest that CaM is a resident RyR2-associated protein anchored at least to residues 3583-3603. This interpretation is consistent with a recent cryo-EM report placing apo- and Ca-CaM at the same location within the RyR2 map.<sup>46</sup> However, we cannot exclude the possibility of beat-to-beat RyR2 regulation by CaM because homozygous RyR2<sup>ADA/ADA</sup> myocytes exhibit prolonged  $\text{Ca}^{2+}$  transient and spark durations. That is consistent with the possible importance of resident CaM for RyR2 shut-off.<sup>13,24,47</sup> During a  $\text{Ca}^{2+}$  transient, RyR2 opening and conformation change could alter anchored CaM function, where binding of  $\text{Ca}^{2+}$  to CaM would facilitate the termination of  $\text{Ca}^{2+}$  release.

## Nearly all Z-line bound CaM is on RyR2

An important finding here is that  $>90\%$  of the total Z-line associated CaM is bound to RyR2, i.e.,  $\sim 1.2\text{ }\mu\text{M}$  (Fig. 1E). This is consistent with our FKBP12.6  $B_{\text{max}}$  measurements,<sup>22</sup> and with the estimated concentration of RyR2 monomers in rat ventricular myocytes,<sup>48</sup> implying that there may be  $\sim 70\text{ nM}$  of non-RyR2 CaM-binding sites at the Z-line. Since the LTCC also binds CaM at the Z-line, and there are  $\sim 32$  RyR2 monomers per LTCC in rat myocytes,<sup>48</sup> LTCC would bind about  $40\text{ nM}$  CaM, consistent with our findings. It is clear that RyR2 is the quantitatively dominant CaM binding site at the Z-line. Total cellular [CaM] in rat cardiac myocytes is  $2\text{-}6\text{ }\mu\text{M}$ , and varies somewhat with species.<sup>49</sup> We infer that a reduction in CaM-RyR2 binding affinity, as in HF or CPVT,<sup>25-27</sup> might also shift CaM's



distribution among different binding targets. Since free [CaM] is only 50-100 nM in myocytes (>95% is bound) even at diastolic  $[Ca^{2+}]_i$ ; there is likely to be competition among target sites for available CaM.<sup>34</sup>

### Defective CaM-RyR2 interaction and SR $Ca^{2+}$ release, CPVT

Here RyR2<sup>ADA/+</sup> mice<sup>13</sup> were used to assess CaM binding at the RyR2 and Z-line quantitatively, but this also alters SR  $Ca^{2+}$  leak which provides a functional correlate. Homozygous RyR2<sup>ADA/ADA</sup> mice have altered SR  $Ca^{2+}$  release, but also exhibit profound HF, death within ~2 weeks of birth, 70% reduction in RyR2 expression T-tubule disorganization.<sup>13,24</sup> Remarkably RyR2<sup>ADA/+</sup> mice have normal lifespan, structure and RyR2 expression with no hypertrophy.<sup>13</sup> This is similar to KI mice carrying a CPVT1 mutation (RyR2-R2474S),<sup>28,50</sup> where heterozygous mice survive without hypertrophy similar to WT, but the homozygous KI is lethal. Decreased CaM-RyR2 binding affinity has also been reported in CPVT1 KI mice under stress conditions known to be arrhythmogenic.<sup>27</sup> Thus, the RyR2<sup>ADA/+</sup> mice studied here resemble a CPVT1 model, and we also assessed abnormal SR  $Ca^{2+}$  release and stress-induced arrhythmic events in these mice.

Baseline  $Ca^{2+}$  transients were similar between RyR2<sup>ADA/+</sup> and WT mice, consistent with prior hemodynamic data, indicating functional normalcy of these mice (vs. WT littermates).<sup>13</sup> RyR2<sup>ADA/+</sup> myocytes exhibited a moderate increase in  $Ca^{2+}$  spark frequency at baseline. The moderate  $Ca^{2+}$  leakiness may explain why the heterozygous mice survive as long as WT controls (unlike homozygous RyR2<sup>ADA/ADA</sup>). Recently, Yamaguchi *et al.*<sup>51</sup> showed that the single RyR2-L3591D mutant (which also reduces RyR2-CaM binding), when homozygous in KI mice, increases RyR2 open probability at diastolic  $[Ca^{2+}]_i$ , but is much better tolerated vs. the RyR2<sup>ADA/ADA</sup> triple mutation. These results are consistent with the CPVT phenotype, where under resting condition the CPVT patients are completely normal.

Catecholamine challenge (ISO) in RyR2<sup>ADA/+</sup> further exacerbated SR  $Ca^{2+}$  leak, limited the ISO-induced lusitropy and SR  $Ca^{2+}$  loading, but the Ca transients were still similarly enhanced (vs. WT; Fig 5). We infer that this is because there is fractional SR  $Ca^{2+}$  release in the RyR2<sup>ADA/+</sup> mice with ISO. So this mouse seems adapted to have normal adrenergic inotropic response, but the SR is pushed closer to instability. In particular, we suspect that the limited lusitropic effect and reduced SR  $Ca^{2+}$  content after ISO in RyR2<sup>ADA/+</sup> mice may be due to the dramatically increased SR  $Ca^{2+}$  leak, especially because Yamaguchi *et al.*<sup>13</sup> found SR Ca-ATPase-dependent uptake rate in RyR2<sup>ADA/+</sup> mice was normal. That agrees with single-channel RyR2 recordings suggesting that defective CaM-RyR2 interaction delays RyR2 closure.<sup>23</sup>

Despite the relative normalcy of  $Ca^{2+}$  transients in RyR2<sup>ADA/+</sup> myocytes, the exacerbation of leak may limit maximal SR  $Ca^{2+}$  content, just as seen for both ISO treatment alone and HF alone.<sup>25,39</sup> This might limit cardiac reserve. More importantly, this enhanced leak in RyR2<sup>ADA/+</sup> increases  $Ca^{2+}$  waves and triggered activity in myocytes and whole animal arrhythmias in response to catecholamine challenge (Fig 4, 6 and 7). This again recapitulates the situation in CPVT1 KI mice and patients.<sup>28,29</sup> In particular, the bidirectional VT seen in

RyR2<sup>ADA/+</sup> (but not WT mice) is clinically diagnostic for CPVT.<sup>29</sup> Although this RyR2 ADA mutation is not a known disease-linked mutation in humans, it causes a CPVT-like phenotype. There are also two recent CaM mutations that are associated with CPVT in patients,<sup>30</sup> and the CPVT phenotype may well result from effects of these mutant CaMs analogous to our RyR2<sup>ADA/+</sup> mouse results here.

We cannot exclude the possibility that the ADA triple mutation alters RyR2 domain interactions, which might also contribute to the functional effects observed. However, the similarity between the RyR2<sup>ADA/+</sup> and simply depleting CaM from the WT RyR2 (Online Fig V) convinces us that the loss of CaM binding is the major factor in RyR2<sup>ADA/+</sup> mice causing abnormal SR Ca<sup>2+</sup> leak and arrhythmias. We recently also showed that CaM binding can stabilize RyR2 conformation in a more stably closed (zipped) state where access of an unzipping peptide is suppressed.<sup>52</sup>

### CaM-RyR2 binding affinity in HF myocytes

Prior work in HF rabbit and canine models demonstrated reduced RyR2-bound CaM, based on co-immunoprecipitation and biochemical analysis,<sup>25,26</sup> but total CaM expression was unaltered.<sup>25</sup> Here we directly measured CaM and FKBP12.6 affinity for RyR2 in situ in HF myocytes. We found a three-fold lower CaM affinity in HF myocytes, while FKBP12.6 affinity was unaltered. This quantitative information allows novel inferences. Assuming that free [CaM] in HF myocytes is 50-100 nM,<sup>34</sup> the saturation of RyR2 monomers with CaM would be expected to drop from 70-90% to 50-70% in HF. This lower RyR2 saturation with CaM may have an analogous functional effect to those that we found in the RyR2<sup>ADA/+</sup> mice, where only 50% of RyR2 can bind CaM. The implication is that reduced CaM binding to RyR2 may contribute to the known increased SR Ca<sup>2+</sup> leak in HF,<sup>4,25</sup> and to the incidence of arrhythmias, which are responsible for 50% of HF deaths.<sup>1</sup> Furthermore, attenuated CaM-RyR2 association in HF could allow other intracellular CaM targets of lower affinity to be better activated, since RyR2 is a major CaM site in myocytes.<sup>11</sup> One such site is CaMKII which is activated in HF and contributes to SR Ca<sup>2+</sup> leak and arrhythmogenesis by phosphorylation and activation of RyR2.<sup>25</sup> Thus, decreased CaM-RyR2 association in HF may synergize with other regulatory pathways to exacerbate cardiac dysfunction and arrhythmias.

Overall, the HF-associated SR Ca<sup>2+</sup> leak is a complicated process involving several factors (e.g., CaM, CaMKII, FKBP12.6, redox modification, etc.). Here, for the first time, we measured directly the in situ binding affinity of RyR2 for FKBP12.6 in HF myocytes, but found it to be unaltered vs. control. We conclude that CaM binding to RyR2 may be an important physiological regulator of RyR2 gating in cardiac myocytes, and that defects in this binding in HF or CPVT might constitute an important molecular mechanism of triggered arrhythmias suitable for therapeutic targeting.

### Supplementary Material

Refer to Web version on PubMed Central for supplementary material.

## Acknowledgments

### SOURCES OF FUNDING

Supported by NIH grants R01-HL092097 (DMB, RLC), P01-HL080101 (DMB), and R01-HL073051 (GM), and by Banyu Life Science Foundation International (TO).

## Nonstandard Abbreviations and Acronyms

$\tau$	time constant
AC	adenylyl cyclase
ADA	W3587A/L3591D/F3603A triple mutation of RyR2
AIP	autocamtide-2 related inhibitory peptide
a.u.	arbitrary units
$B_{\max}$	binding maximum
CaM	calmodulin
CaMK	Ca <sup>2+</sup> /CaM-dependent kinase
CaN	calcineurin
CPVT	catecholaminergic polymorphic ventricular tachycardia
VT	ventricular tachycardia
DAD	delayed afterdepolarization
EAF	enhanced acceptor fluorescence
F	fluorescent
FDHM	full duration at half maximum
FKBP12.6	FK506 binding protein
FRAP	fluorescence recovery after photobleaching
FRET	fluorescence resonance energy transfer
FRET <sub>max</sub>	FRET value at saturating acceptor concentration.
FWHM	full width at half maximum
HF	heart failure
ISO	isoproterenol
$K_d$	dissociation constant
KI	knock-in
$k_{\text{off}}$	dissociation rate constant
$k_{\text{on}}$	association rate constant
LTCC	L-type calcium channels

<b>LVDD</b>	left ventricular diastolic dimension
<b>LVSD</b>	left ventricular systolic dimension
<b>MI</b>	myocardial infarction
<b>NCX</b>	Na/Ca exchanger
<b>NOS</b>	nitric oxide synthase
<b>NT</b>	normal Tyrode's solution
<b>PDE</b>	phosphodiesterase
<b>RyR2</b>	cardiac ryanodine receptor
<b>SE</b>	sensitized emission
<b>SR</b>	sarcoplasmic reticulum

## REFERENCES

1. Noseworthy PA, Newton-Cheh C. Genetic determinants of sudden cardiac death. *Circulation*. 2008; 118:1854–1863. [PubMed: 18955676]
2. Vermeulen JT, McGuire MA, Opthof T, Coronel R, Bakker JM, Klöpping C, Janse MJ. Triggered activity and automaticity in ventricular trabeculae of failing human and rabbit hearts. *Cardiovasc Res*. 1994; 28:1547–1554. [PubMed: 8001044]
3. Pogwizd SM, Bers DM. Cellular basis of triggered arrhythmias in heart failure. *Trends Cardiovasc Med*. 2004; 14:61–66. [PubMed: 15030791]
4. Shannon TR, Pogwizd SM, Bers DM. Elevated sarcoplasmic reticulum Ca<sup>2+</sup> leak in intact ventricular myocytes from rabbits in heart failure. *Circ Res*. 2003; 93:592–594. [PubMed: 12946948]
5. Pogwizd SM, Bers DM. Na/Ca exchange in heart failure: contractile dysfunction and arrhythmogenesis. *Ann NY Acad Sci*. 2002; 976:454–465. [PubMed: 12502595]
6. Bers DM, Pogwizd SM, Schlotthauer K. Upregulated Na/Ca exchange is involved in both contractile dysfunction and arrhythmogenesis in heart failure. *Basic Res Cardiol*. 2002; 97:136–42. [PubMed: 12479232]
7. Jurado LA, Chockalingam PS, Jarrett HW. Apocalmodulin. *Physiol Rev*. 1999; 79:661–682. [PubMed: 10390515]
8. Means AR, VanBerkum MF, Bagchi I, Lu KP, Rasmussen CD. Regulatory functions of calmodulin. *Pharmacol Ther*. 1991; 50:255–270. [PubMed: 1763137]
9. Vogel HJ. Calmodulin: a versatile calcium mediator protein. *Biochem Cell Biol*. 1994; 72:357–376. [PubMed: 7605608]
10. James PT, Vorherr EC. Calmodulin-binding domains: just two faced or multi-faceted? *Trends Biochem Sci*. 1995; 20:38–42. [PubMed: 7878743]
11. Maier LS, Bers DM. Calcium, calmodulin, and calcium-calmodulin kinase II: heartbeat to heartbeat and beyond. *J Mol Cell Cardiol*. 2002; 34:919–939. [PubMed: 12234763]
12. Yamaguchi N, Xu L, Pasek DA, Evans KE, Meissner G. Molecular basis of calmodulin binding to cardiac muscle Ca<sup>2+</sup> release channel (ryanodine Receptor). *J Biol Chem*. 2003; 278:23480–23486. [PubMed: 12707260]
13. Yamaguchi N, Takahashi N, Xu L, Smithies O, Meissner G. Early cardiac hypertrophy in mice with impaired calmodulin regulation of cardiac muscle Ca release channel. *J Clin Invest*. 2007; 117:1344–1353. [PubMed: 17431507]

14. Balshaw DM, Xu L, Yamaguchi N, Pasek DA, Meissner G. Calmodulin binding and inhibition of cardiac muscle calcium release channel (ryanodine receptor). *J Biol Chem.* 2001; 276:20144–20153. [PubMed: 11274202]
15. Moore CP, Rodney G, Zhang JZ, Santacruz-Tolosa L, Strasburg G, Hamilton SL. Apocalmodulin and Ca<sup>2+</sup> Calmodulin Bind to the Same Region on the Skeletal Muscle Ca<sup>2+</sup> Release Channel. *Biochemistry.* 1999; 38:8532–8537. [PubMed: 10387100]
16. Wagenknecht T, Berkowitz J, Grassucci R, Timerman AP, Fleischer S. Localization of calmodulin binding sites on the ryanodine receptor from skeletal muscle by electron microscopy. *Biophys J.* 1994; 67:2286–2295. [PubMed: 7696469]
17. Cornea RL, Nitu F, Gruber S, Kohler K, Satzer M, Thomas DD, Fruen BR. FRET-based mapping of calmodulin bound to the RyR1 Ca<sup>2+</sup> release channel. *Proc Natl Acad Sci USA.* 2009; 106:6128–6133. [PubMed: 19332786]
18. Guo T, Fruen BR, Nitu FR, Nguyen TD, Yang Y, Cornea RL, Bers DM. FRET detection of calmodulin binding to the cardiac RyR2 calcium release channel. *Biophys J.* 2011; 101:2170–2177. [PubMed: 22067155]
19. Marx SO, Reiken S, Hisamatsu Y, Jayaraman T, Burkhoff D, Rosemblyt N, Marks AR. PKA phosphorylation dissociates FKBP12.6 from the calcium release channel (ryanodine receptor): defective regulation in failing hearts. *Cell.* 2000; 101:365–376. [PubMed: 10830164]
20. Wehrens XH, Lehnart SE, Reiken S, van der Nagel R, Morales R, Sun J, Cheng Z, Deng SX, de Windt LJ, Landry DW, Marks AR. Enhancing calstabin binding to ryanodine receptors improves cardiac and skeletal muscle function in heart failure. *Proc Natl Acad Sci U S A.* 2005; 102:9607–9612. [PubMed: 15972811]
21. Barg S, Copello JA, Fleischer S. Different interactions of cardiac and skeletal muscle ryanodine receptors with FK-506 binding protein isoforms. *Am J Physiol.* 1997; 272:1726–1733.
22. Guo T, Cornea RL, Huke S, Camors E, Yang Y, Picht E, Fruen BR, Bers DM. Kinetics of FKBP12.6 binding to ryanodine receptors in permeabilized cardiac myocytes and effects on ca sparks. *Circ Res.* 2010; 106:1743–1752. [PubMed: 20431056]
23. Xu L, Meissner G. Mechanism of calmodulin inhibition of cardiac sarcoplasmic reticulum Ca<sup>2+</sup> release channel (ryanodine receptor). *Biophys J.* 2004; 86:797–804. [PubMed: 14747315]
24. Arnáiz-Cot JJ, Damon BJ, Zhang XH, Cleemann L, Yamaguchi N, Meissner GW, Morad M. Cardiac calcium signaling pathologies associated with defective calmodulin regulation of type 2 ryanodine receptor. *J Physiol.* 2013; 591:4287–4299. [PubMed: 23836685]
25. Ai X, Curran JW, Shannon TR, Bers DM, Pogwizd SM. Ca<sup>2+</sup>/calmodulin-dependent protein kinase modulates cardiac ryanodine receptor phosphorylation and sarcoplasmic reticulum Ca<sup>2+</sup> leak in heart failure. *Circ Res.* 2005; 97:1314–1322. [PubMed: 16269653]
26. Ono M, Yano M, Hino A, Suetomi T, Xu J, Susa T, Uchinoumi H, Tateishi H, Oda T, Okuda S, Doi M, Kobayashi S, Yamamoto T, Koseki N, Kyushiki H, Ikemoto N, Matsuzaki M. Dissociation of calmodulin from cardiac ryanodine receptor causes aberrant Ca<sup>2+</sup> release in heart failure. *Cardiovasc Res.* 2010; 87:609–617. [PubMed: 20388639]
27. Xu X, Yano M, Uchinoumi H, Hino A, Suetomi T, Ono M, Tateishi H, Oda T, Okuda S, Doi M, Kobayashi S, Yamamoto T, Ikeda Y, Ikemoto N, Matsuzaki M. Defective calmodulin binding to the cardiac ryanodine receptor plays a key role in CPVT-associated channel dysfunction. *Biochem Biophys Res Commun.* 2010; 394:660–6. [PubMed: 20226167]
28. Uchinoumi H, Yano M, Suetomi T, Ono M, Xu X, Tateishi H, Oda T, Okuda S, Doi M, Kobayashi S, Yamamoto T, Ikeda Y, Ohkusa T, Ikemoto N, Matsuzaki M. Catecholaminergic polymorphic ventricular tachycardia is caused by mutation-linked defective conformational regulation of the ryanodine receptor. *Circ Res.* 2010; 106:1413–1424. [PubMed: 20224043]
29. Priori SG, Napolitano C, Memmi M, Colombi B, Drago F, Gasparini M, DeSimone L, Coltorti F, Bloise R, Keegan R, Cruz Filho FE, Vignati G, Benatar A, DeLogu A. Clinical and Molecular Characterization of Patients with Catecholaminergic Polymorphic Ventricular Tachycardia. *Circulation.* 2002; 106:69–74. [PubMed: 12093772]
30. Nyegaard M, Overgaard MT, Søndergaard MT, Vranas M, Behr ER, Hildebrandt LL, Lund C, Hedley PL, Camm AJ, Wettrell G, Fosdal I, Christiansen M, Børghlum AD. Mutations in

Calmodulin Cause Ventricular Tachycardia and Sudden Cardiac Death. *American Journal of Human Genetics*. 2012; 91:703–712. [PubMed: 23040497]

31. Tanonaka K, Furuhashi KI, Yoshida H, Kakuta K, Miyamoto Y, Toga W, Takeo S. Protective effect of heat shock protein 72 on contractile function of perfused failing heart. *Am J Physiol*. 2001; 281:215–222.
32. Lin L, Kim SC, Wang Y, Gupta S, Davis B, Simon SI, Torre-Amione G, Knowlton AA. HSP60 in heart failure: abnormal distribution and role in cardiac myocyte apoptosis. *Am J Physiol*. 2007; 293:2238–2247.
33. Van Oort RJ, McCauley MD, Dixit SS, Pereira L, Yang Y, Respress JL, Wang Q, De Almeida AC, Skapura DG, Anderson ME, Bers DM, Wehrens XH. Ryanodine receptor phosphorylation by calcium/calmodulin-dependent protein kinase II promotes life-threatening ventricular arrhythmias in mice with heart failure. *Circulation*. 2010; 122:2669–2679. [PubMed: 21098440]
34. Wu X, Bers DM. Free and bound intracellular calmodulin measurements in cardiac myocytes. *Cell Calcium*. 2007; 41:353–64. [PubMed: 16999996]
35. Kelly EM, Hou Z, Bossuyt J, Bers DM, Robia SL. Phospholamban Oligomerization, Quaternary structure, and sarco(endo)plasmic reticulum calcium ATPase binding measured by fluorescence resonance energy transfer in living cells. *J Biol Chem*. 2008; 283:12202–12211. [PubMed: 18287099]
36. Song Q, Saucerman JJ, Bossuyt J, Bers DM. Differential integration of Ca<sup>2+</sup>-calmodulin signal in intact ventricular myocytes at low and high affinity Ca<sup>2+</sup>-calmodulin targets. *J Bio Chem*. 2008; 283:31531–31540. [PubMed: 18790737]
37. Zima A, Bovo E, Bers DM, Blatter LA. Properties of sarcoplasmic reticulum Ca<sup>2+</sup> leak in normal and failing rabbit ventricular myocytes. *J Physiol*. 2010; 588:4743–475. [PubMed: 20962003]
38. Guo T, Zhang T, Ginsburg KS, Mishra S, Brown JH, Bers DM. CaMKII $\delta_C$  slows [Ca]<sub>i</sub> decline in cardiac myocytes by promoting Ca sparks. *Biophys J*. 2012; 102:2461–2470. [PubMed: 22713561]
39. Curran J, Ríos E, Bers DM, Shannon TR.  $\beta$ -adrenergic enhancement of sarcoplasmic reticulum Ca leak in cardiac myocytes is mediated by Ca-calmodulin-dependent protein kinase. *Circ. Res*. 2007; 100:391–398. [PubMed: 17234966]
40. Cerrone M, Colombi B, Santoro M, di Barletta MR, Scelsi M, Villani L, Napolitano C, Priori SG. Bidirectional ventricular tachycardia and fibrillation elicited in a knock-in mouse model carrier of a mutation in the cardiac ryanodine receptor. *Circ Res*. 2005; 96:e77–82. [PubMed: 15890976]
41. Bers DM. Ryanodine receptor S2808 phosphorylation in heart failure: smoking gun or red herring. *Circ Res*. 2012; 110:796–799. [PubMed: 22427320]
42. Guo T, Zhang T, Mestral R, Bers DM. Ca/calmodulin-dependent protein kinase II phosphorylation of ryanodine receptor does affect calcium sparks in mouse ventricular myocytes. *Circ Res*. 2006; 99:398–406. [PubMed: 16840718]
43. Balog EM, Norton LE, Thomas DD, Fruen BR. Role of calmodulin methionine residues in mediating productive association with cardiac ryanodine receptors. *Am J Physiol*. 2006; 290:794–799.
44. Tripathy A, Xu L, Mann G, Meissner G. Calmodulin activation and inhibition of skeletal muscle Ca<sup>2+</sup> release channel (ryanodine receptor). *Biophys J*. 1995; 69:106–119. [PubMed: 7669888]
45. Samsó M, Wagenknecht T. Apocalmodulin and Ca<sup>2+</sup>-calmodulin bind to neighboring locations on the ryanodine receptor. *J Bio Chem*. 2002; 277:1349–1353. [PubMed: 11694536]
46. Huang X, Fruen BR, Farrington DT, Wagenknecht T, Liu Z. Calmodulin-binding locations on the skeletal and cardiac ryanodine receptors. *J Biol Chem*. 2012; 287:30328–30335. [PubMed: 22773841]
47. Tian X, Tang Y, Wang R, Chen SRW. Calmodulin modulates the termination threshold for cardiac ryanodine receptor-mediated Ca<sup>2+</sup> release. *Biochem J*. 2013:367–375. [PubMed: 23992453]
48. Bers DM, Stiffel VM. Ratio of ryanodine to dihydropyridine receptors in cardiac and skeletal muscle and implications for E-C coupling. *Am J Physiol*. 1993; 264:1587–1593.
49. Maier LS, Ziolo MT, Bossuyt J, Persechini A, Mestral R, Bers DM. Dynamic changes in free Ca-calmodulin levels in adult cardiac myocytes. *J Mol Cell Cardiol*. 2006; 41:451–458. [PubMed: 16765983]

50. Lehnart SE, Mongillo M, Bellinger A, Lindegger N, Chen BX, Hsueh W, Reiken S, Wronska A, Drew LJ, Ward CW, Lederer WJ, Kass RS, Morley G, Marks AR. Leaky  $\text{Ca}^{2+}$  release channel/ryanodine receptor 2 causes seizures and sudden cardiac death in mice. *J Clin Invest*. 2008; 118:2230–2245. [PubMed: 18483626]
51. Yamaguchi N, Chakraborty A, Huang TQ, Xu L, Gomez AC, Pasek DA, Meissner G. Cardiac hypertrophy associated with impaired regulation of cardiac ryanodine receptor by calmodulin and S100A1. *Am J Physiol Heart Circ Physiol*. 2013; 305:H86–94. [PubMed: 23666671]
52. Oda T, Yang Y, Nitu RF, Svensson B, Lu X, Fruen RB, Cornea LR, Bers DM. In Cardiomyocytes, Binding of Unzipping Peptide Activates Ryanodine Receptor 2 and Reciprocally Inhibits Calmodulin Binding. *Circ Res*. 2013; 112:487–497. [PubMed: 23233753]

## Novelty and Significance

### *What Is Known?*

- Calmodulin (CaM) binds to multiple cellular targets, including the SR Ca<sup>2+</sup> release channel (RyR2) in cardiomyocytes. CaM binding reduces RyR channel opening and can reduce SR Ca<sup>2+</sup> leakiness.
- Abnormal SR Ca<sup>2+</sup> leak is thought to contribute to dysfunction and arrhythmias in CPVT (Catecholaminergic polymorphic ventricular tachycardia) and heart failure (HF).
- FK506-binding protein 12.6 (FKBP12.6) binds to RyR2 with high affinity and may also stabilize RyR gating, but results are controversial.

### *What New Information Does This Article Contribute?*

- In the native cardiac myocyte environment with 50 nM [Ca<sup>2+</sup>]<sub>i</sub>, CaM binds to RyR2 (and at the Z-line) with high affinity (K<sub>d</sub> = ~ 15 nM).
- More than 90% of the CaM at the Z-line is RyR2 bound in cardiac myocytes.
- CaM dissociation from RyR2 or lack of binding to mutant RyR2 can lead to abnormal SR Ca release in the form of increased Ca sparks, Ca waves, triggered activity and arrhythmias at the whole animal level.
- These arrhythmogenic features recapitulate RyR2 changes seen in CPVT and HF.
- In a post-myocardial infarction rat HF model, RyR2-CaM binding affinity is reduced ~3 fold, while FKBP12.6 affinity is unaltered.

CaM is known as a mediator of Ca<sup>2+</sup> signals, and it can bind to and alter RyR properties. However, little quantitative data are available about CaM-RyR interaction and function in native cardiac myocytes. We used confocal fluorescence microscopy to measure the in situ binding kinetics and affinity of CaM for RyR in normal myocytes and in myocytes from mice expressing a mutant RyR that cannot bind CaM (CPVT-like model) and from rats with post-MI-induced HF. Using fluorescence resonance energy transfer (FRET), we can distinguish RyR2-bound CaM from CaM bound to other sites in the myocyte. More than 90% of the CaM that is already highly concentrated along the Z-lines of the myocyte is bound directly to RyR. We also found that CaM binding to RyR was reduced in the CPVT-like and HF models and it that causes enhanced SR Ca<sup>2+</sup> leak leading to arrhythmogenic events (. Reduced CaM binding to RyR in cardiac myocytes resulting in enhanced SR Ca leak may be an important contributor to both reduced systolic function and arrhythmias.



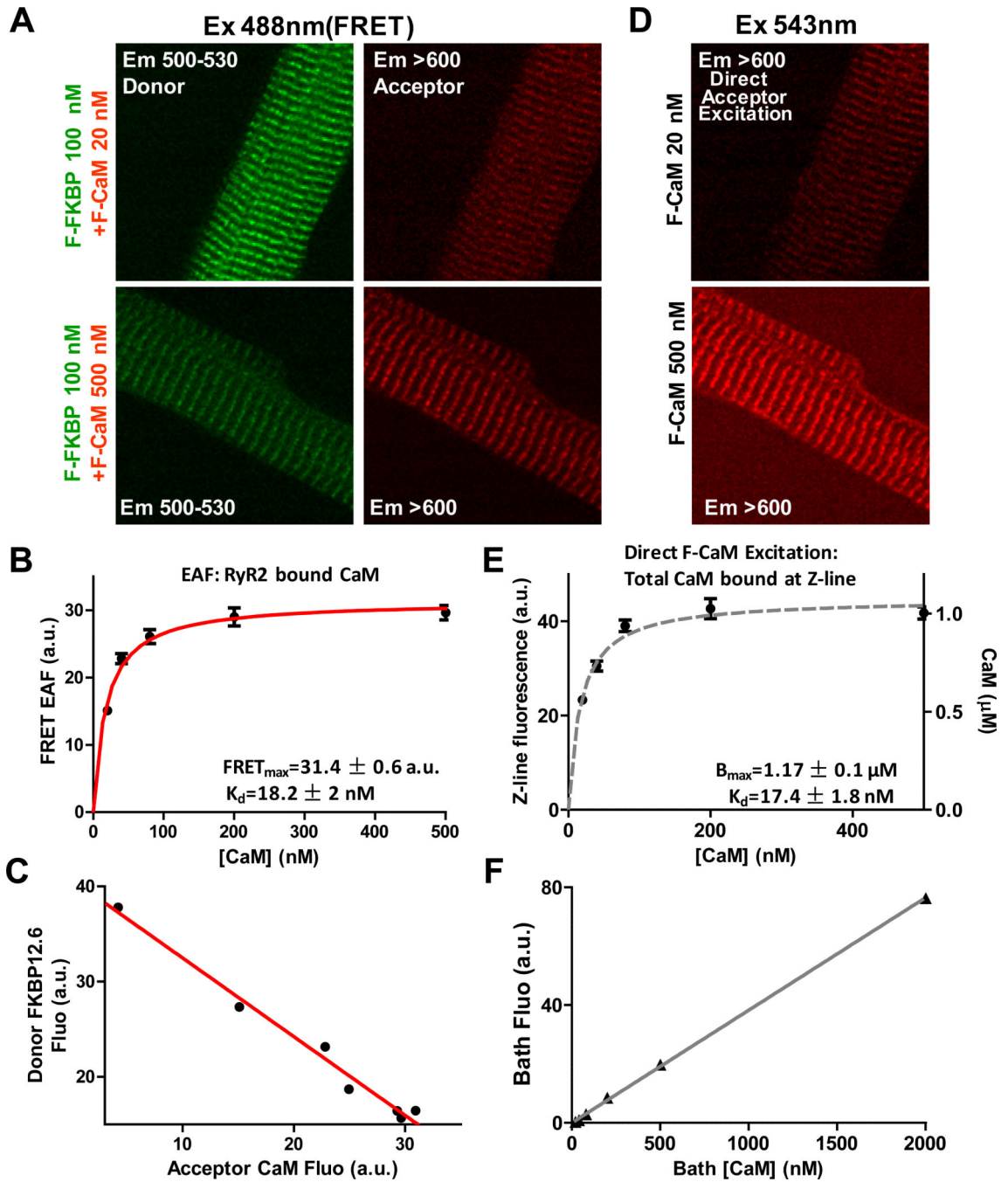


**Figure 1. RyR2 FRET CaM binding and Z-line total CaM binding**

A, FRET images for 20 and 500 nM acceptor [F-CaM], while keeping donor (F-FKBP) saturated. Donor fluorescence decreases and FRET signal increases at higher acceptor [F-CaM]. B, Acceptor (FRET) signal fit with single saturable binding isotherm (n=11-13). C, Donor quench and acceptor FRET are linearly related. D, Z-line images for direct F-CaM excitation at 20 and 500 [F-CaM]. E, binding affinity fitted for CaM at Z-line (n=11-13), reflecting the  $K_d$  and total CaM ( $B_{max}$ ). F, Calibration of F-CaM fluorescence for different bath [F-CaM].

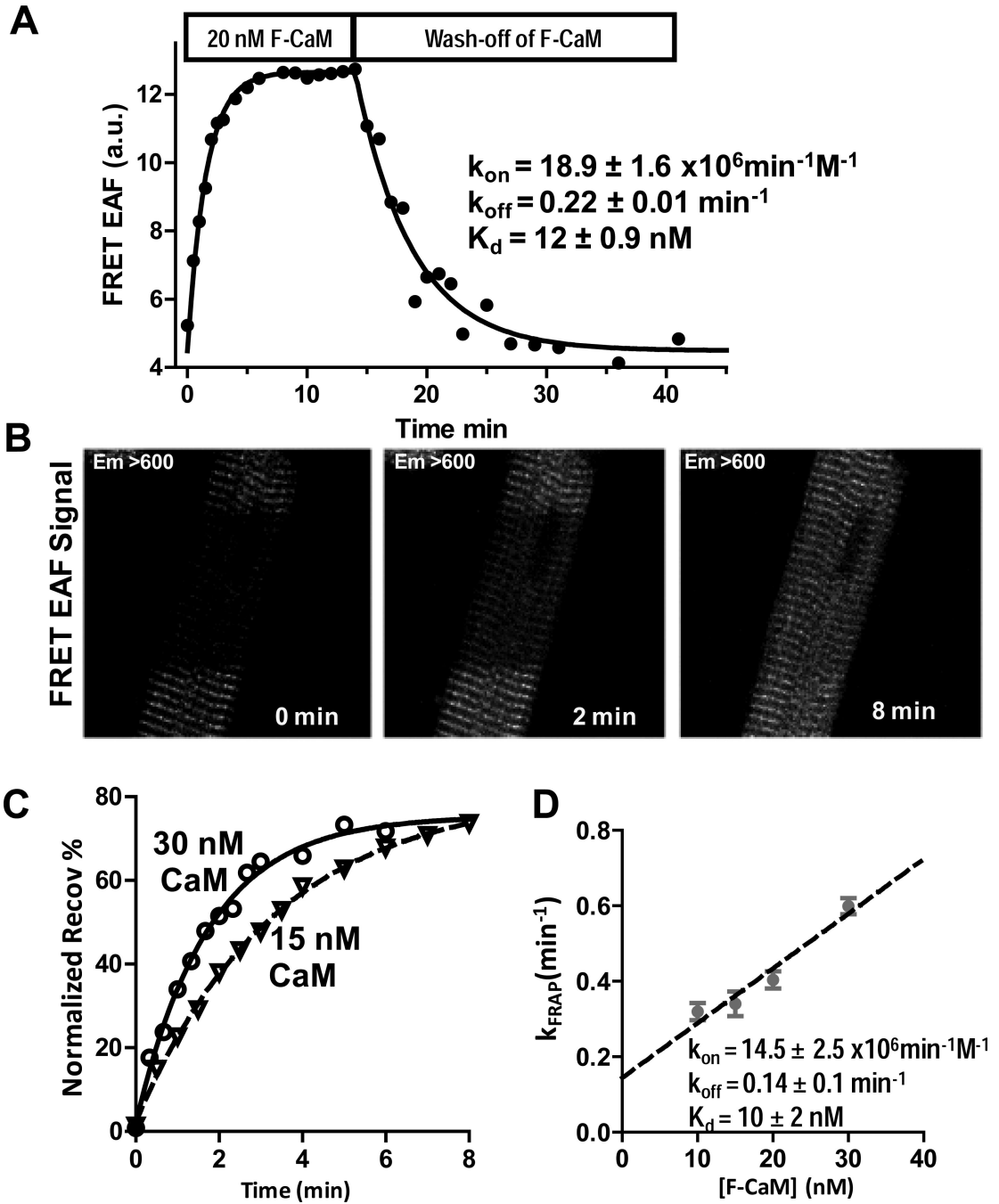


**Figure 2. Binding kinetics of CaM-RyR2**

**A**, Representative time course of FRET (CaM fluorescence upon F-FKBP excitation) for 20nM F-CaM wash-in/off. CaM-RyR2  $k_{on}$ ,  $k_{off}$  and  $K_d$  are indicated (n=5). **B**, Recovery of photobleached FRET striation image in 20 nM [F-CaM] imaged at indicated times. **C**, FRAP rate constants ( $k_{FRAP}$ ; single-exponential fits) at 15 and 30 nM F-CaM. **D**,  $k_{on}$  (slope) and  $k_{off}$  (intercept) are extracted from linear regression fitting (n=8-10), and  $K_d$  is inferred.

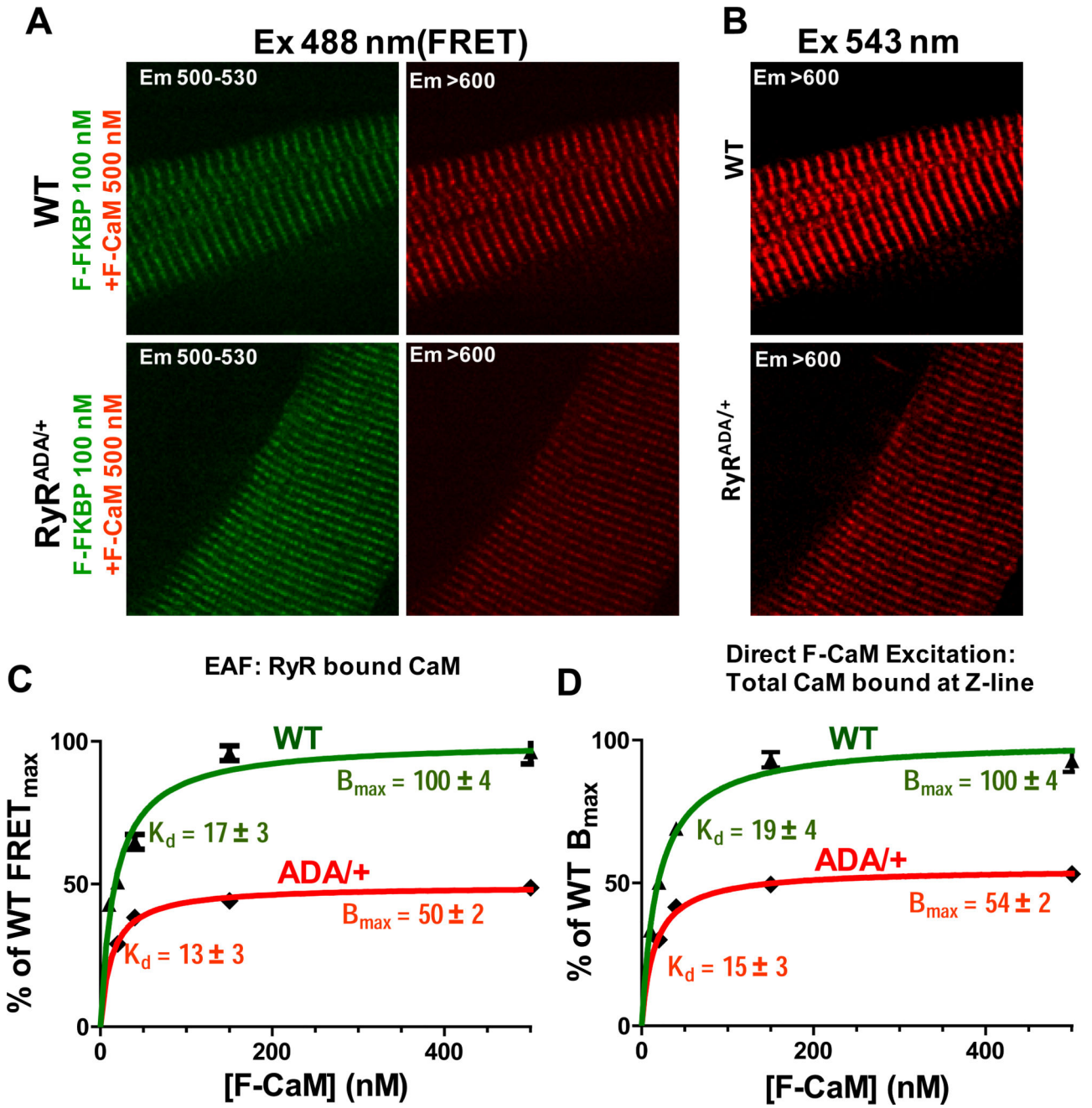


**Figure 3. Percentage of Z-line CaM that is on RyR2**

**A**, FRET images in saturating F-CaM and FFKBP12.6 conditions for WT and RyR2<sup>ADA/+</sup>. **B**, Z-line bound F-CaM images (direct F-CaM excitation) for WT and RyR2<sup>ADA/+</sup>. **C**, Steady state CaM binding, with  $B_{max}$  normalized to WT level and with  $K_d$  inferred (n=12-20). **D**, Total Z-line associated F-CaM with  $B_{max}$  and  $K_d$  for RyR2<sup>ADA/+</sup> and WT mice (n=14-20).

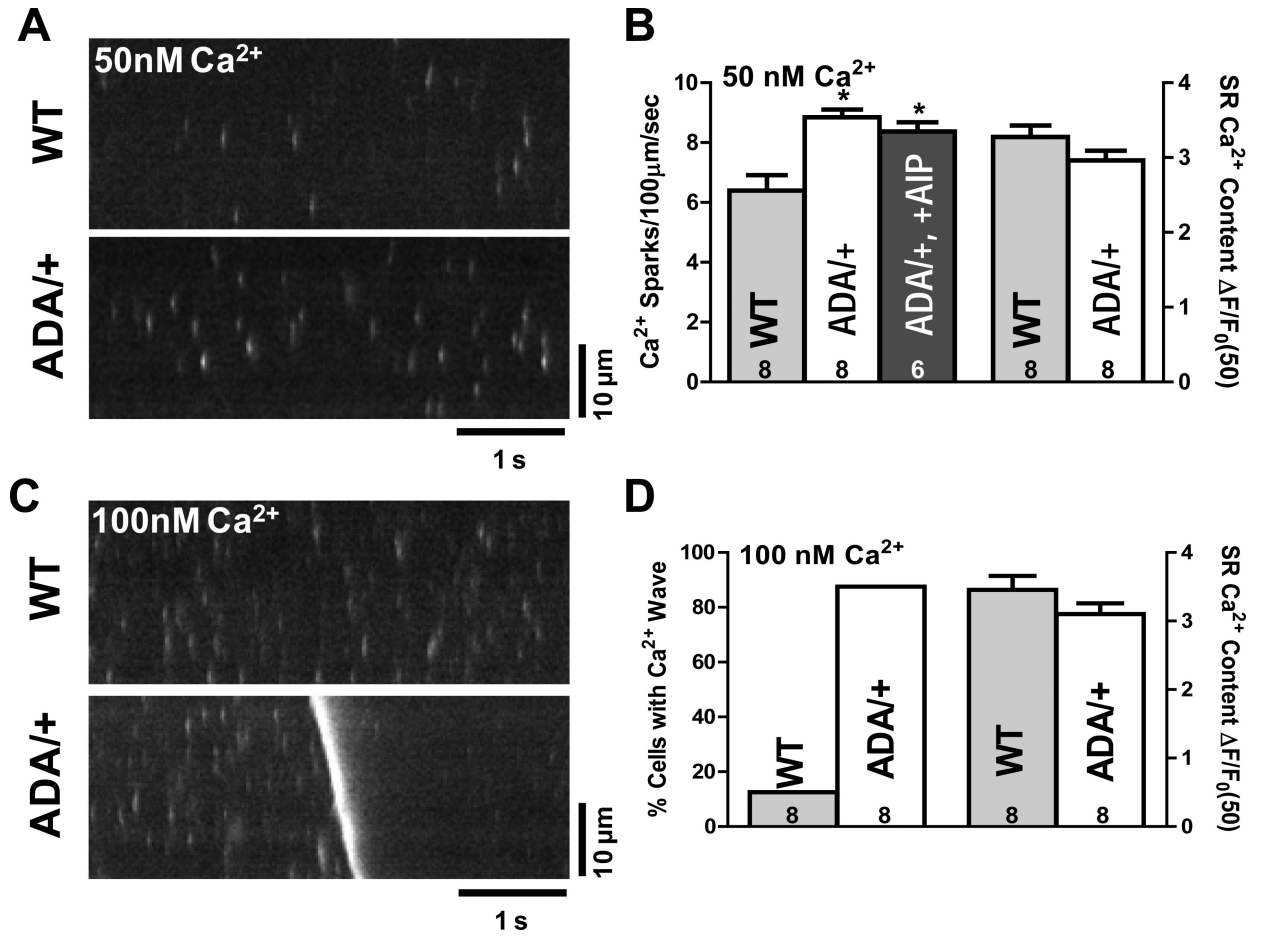


**Figure 4. Diastolic Ca<sup>2+</sup> leak in permeabilized myocytes**

**A**, Confocal line images of Ca<sup>2+</sup> sparks for 50nM [Ca<sup>2+</sup>] in WT and RyR<sup>ADA/+</sup> mice. **B**, Mean Ca<sup>2+</sup> spark frequency and SR Ca<sup>2+</sup> content for WT and RyR<sup>ADA/+</sup> mice (±CaMKII inhibitor AIP). **C**, Confocal line scan at 100nM [Ca<sup>2+</sup>], showing a Ca<sup>2+</sup> wave for RyR<sup>ADA/+</sup>, but not for WT mouse. **D**, Percentage of myocytes showing Ca<sup>2+</sup> waves and SR Ca<sup>2+</sup> content for WT and RyR<sup>ADA/+</sup> mice.

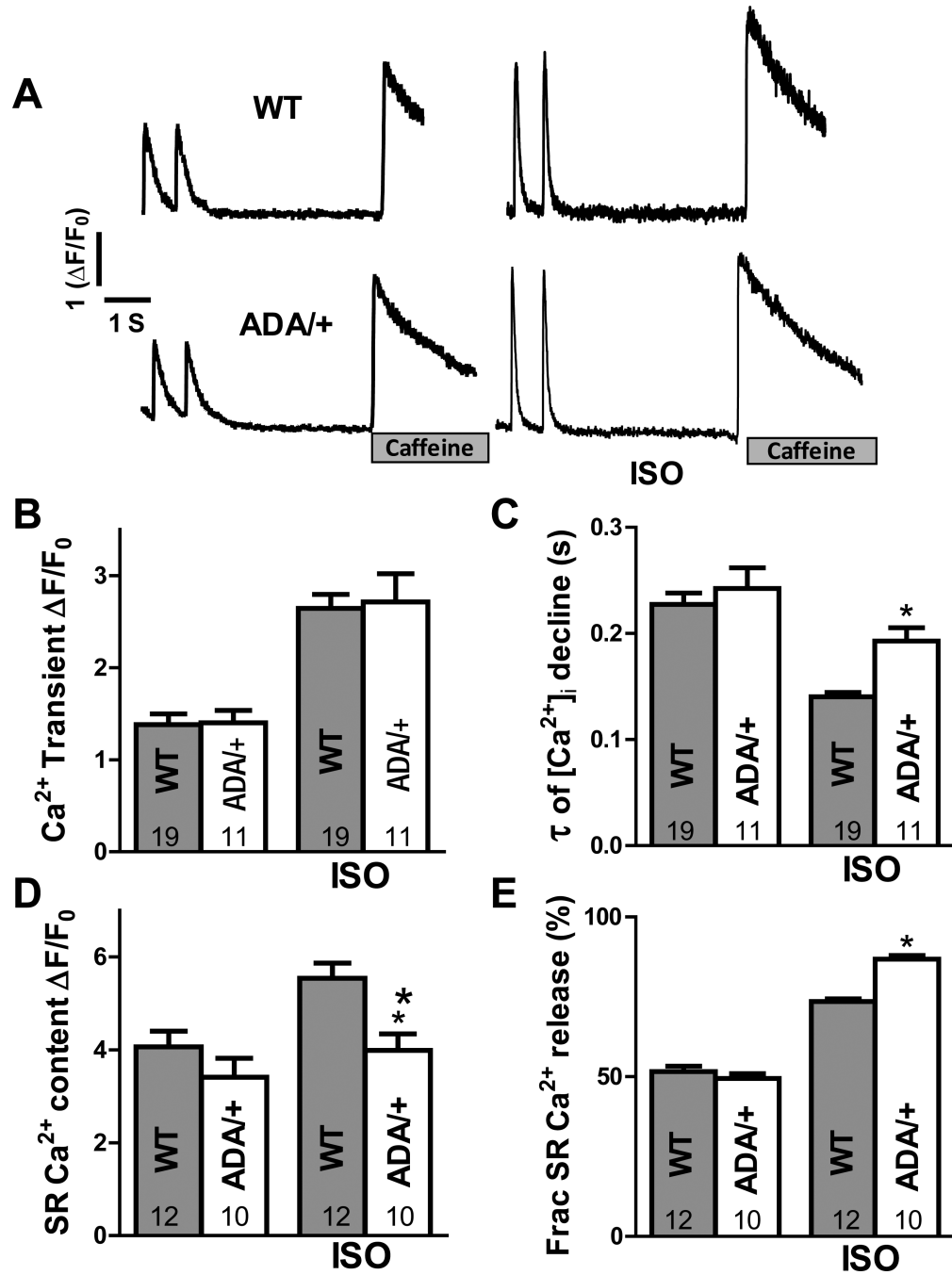


**Figure 5.  $Ca^{2+}$  transients in intact myocytes**

**A**, Representative  $Ca^{2+}$  transients and SR  $Ca^{2+}$  content (assessed by 10 mM caffeine exposure) during at 1 Hz stimulation with and without isoproterenol (ISO; 50nM) for WT and RyR2<sup>ADA/+</sup> mice. **B**, Average twitch transients amplitude ( $\Delta F/F_0$ ). **C**, time constant of twitch  $[Ca^{2+}]_i$  decline. **D**, SR  $Ca^{2+}$  content (amplitude of caffeine-induced Ca transient). **E**, Fractional SR  $Ca^{2+}$  release (ratio for twitch  $Ca^{2+}$  transient amplitude to caffeine-induced  $Ca^{2+}$  release).

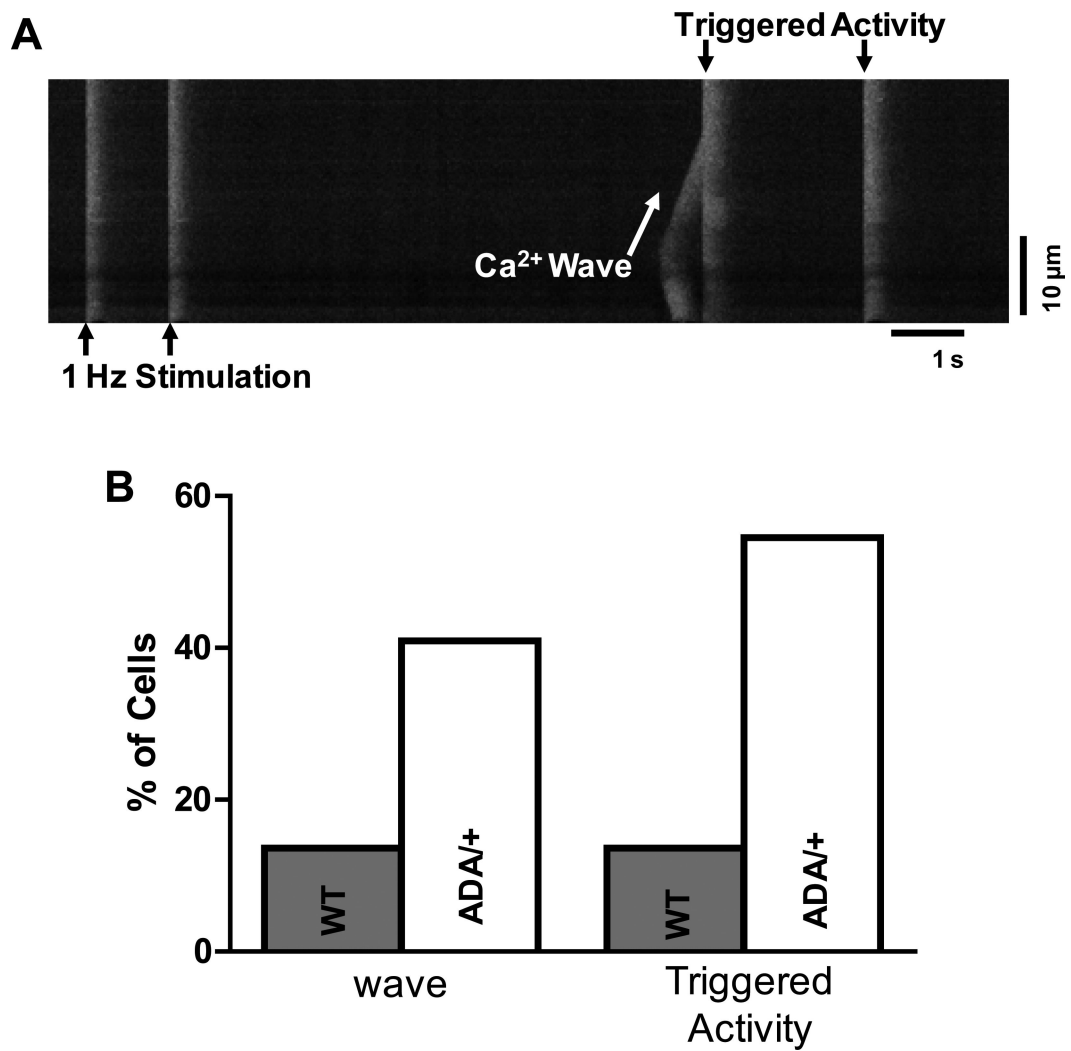


**Figure 6. Arrhythmogenic  $\text{Ca}^{2+}$  waves in isoproterenol-treated myocytes**

**A**, representative line-scan image of  $\text{Ca}^{2+}$  wave (sloping  $[\text{Ca}^{2+}]$  rise) and triggered activity in intact myocyte with 50 nm ISO. The almost instantaneous spread of SR  $\text{Ca}^{2+}$  release at triggered beats indicates that action potentials were induced. **B**, Percentage of myocytes exhibiting  $\text{Ca}^{2+}$  waves and triggered activity for WT (n=24) and  $\text{RyR}^{\text{ADA}/+}$  (n=22).

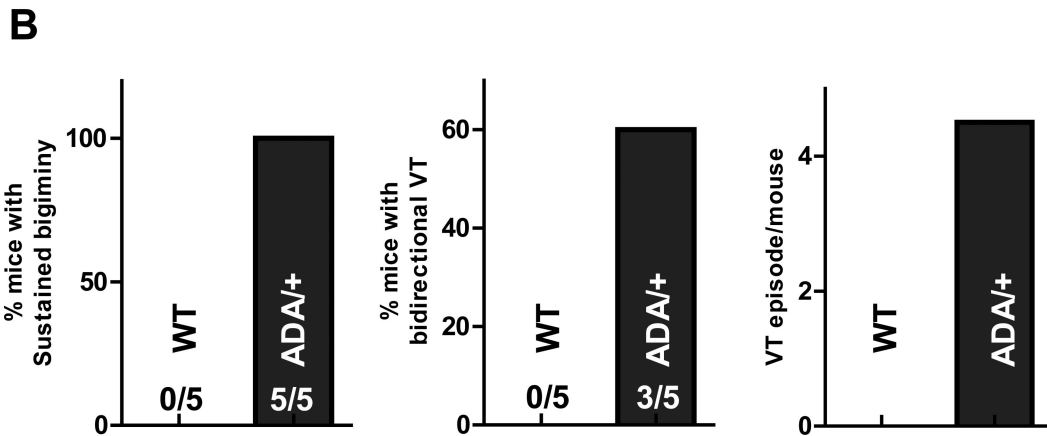
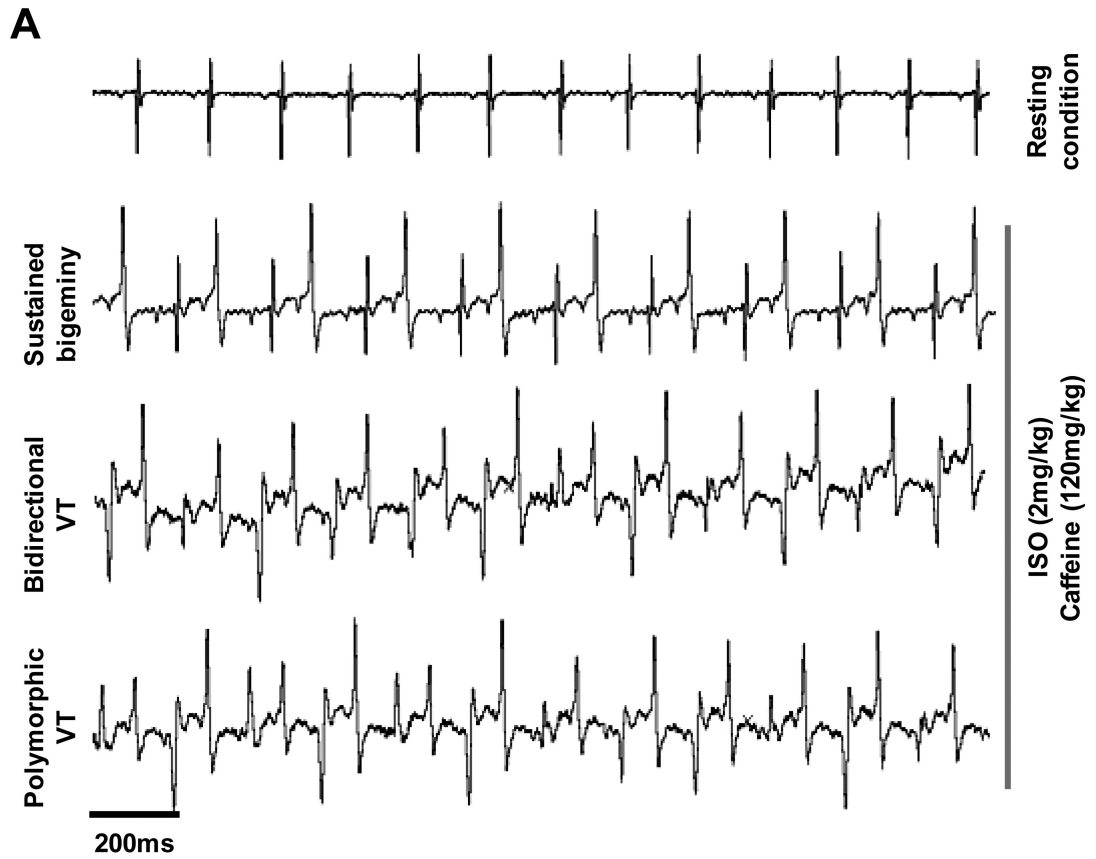


**Figure 7. Effect of caffeine plus ISO on ventricular arrhythmia (RyR2<sup>ADA/+</sup>)**

**A**, representative ECG recording for RyR2<sup>ADA/+</sup> mice, severe ventricular arrhythmia (sustained bigeminy, bidirectional VT and polymorphic VT) were induced by ISO plus caffeine. **B**, 100% of RyR2<sup>ADA/+</sup> mice exhibit sustained bigeminy (> 20min); 60% RyR2<sup>ADA/+</sup> mice exhibit typical bidirectional VT, and VT (bidirectional or polymorphic) episode is 4.5/mouse.

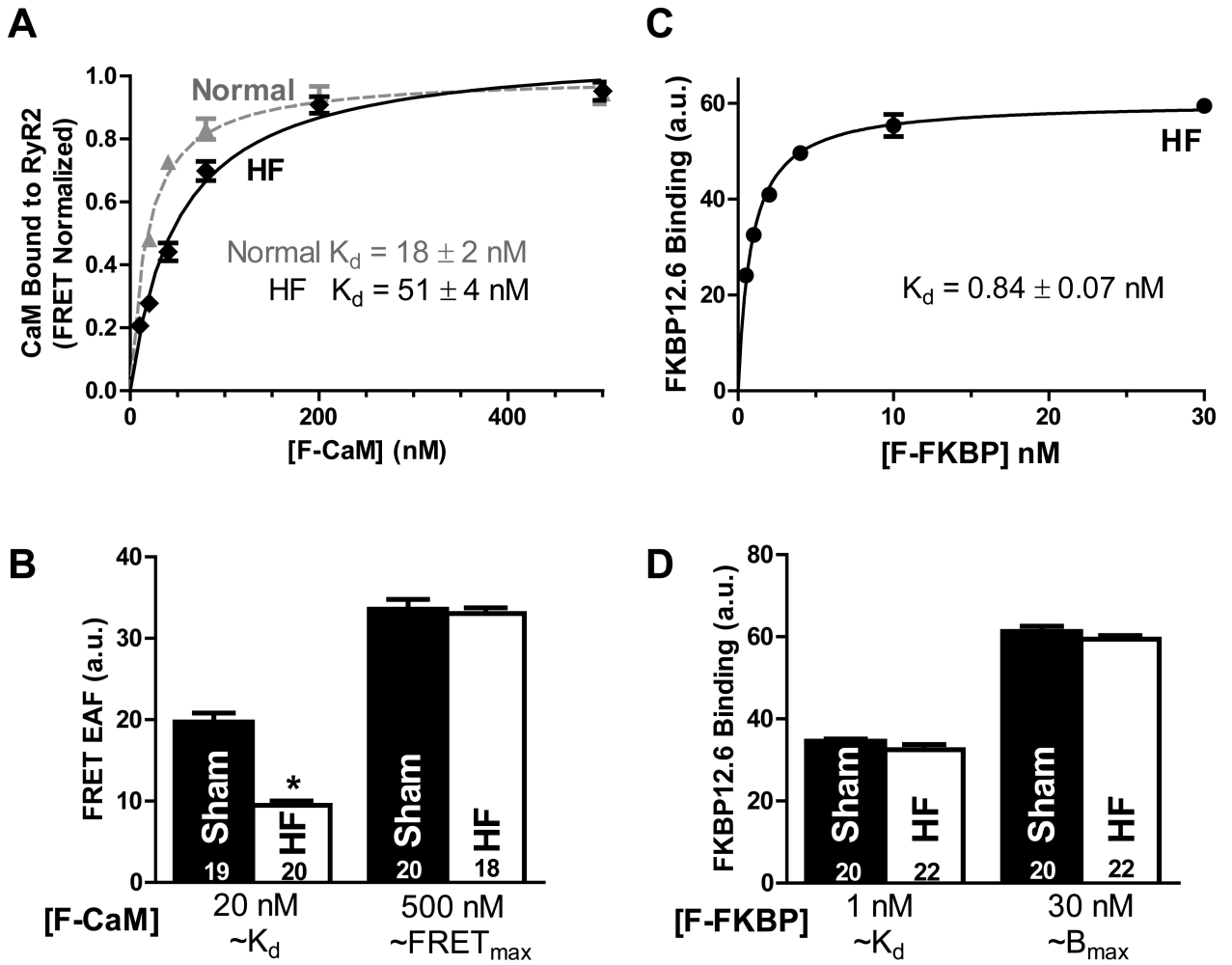


**Figure 8. CaM/FKBP12.6 binding affinity to RyR2 in HF myocytes**

A, FRET detection and steady-state concentration-dependant binding,  $K_d$  of CaM-RyR2 was measured in HF myocytes (n=18). B,  $K_d$  for FKBP12.6-RyR2 was measured by steady-state binding in HF myocytes (n=18-22). C, for  $K_d$  range (20 nM), there is a significant decrease CaM-RyR2 associate rate for HF, but with same  $B_{max}$  (in saturating condition). D, for  $K_d$  range or saturating condition ( $B_{max}$ ), the FKBP12.6-RyR2 associate rate are unchanged for control and HF myocytes